

01.5;06.3

## Control of Chaotic Dark Dissipative Envelope Solitons in an Active Ring Resonator Based on a Magnonic Crystal with a Dynamic Defect

© A.S. Bir<sup>1</sup>, D.V. Romanenko<sup>1</sup>, V.N. Skorokhodov<sup>1</sup>, S.A. Nikitov<sup>1,2</sup>, S.V. Grishin<sup>1</sup>

<sup>1</sup> Saratov National Research State University, Saratov, Russia

<sup>2</sup> Kotelnikov Institute of Radio Engineering and Electronics, Russian Academy of Sciences, Moscow, Russia

E-mail: sergrsh@yandex.ru

Received January 19, 2023

Revised January 30, 2023

Accepted January 30, 2023

Dynamic control of chaotic dark dissipative envelope solitons in a microwave active ring resonator containing two nonlinear elements: a one-dimensional magnonic crystal (MC) with a dynamic linear defect and a transistor amplifier is performed. Dissipative envelope solitons are formed on a long-wavelength surface magnetostatic wave propagating in the MC and parametrically decaying into short-wavelength spin waves. A constant electric current flowing through a copper conductor creates a dynamic linear defect along the longitudinal axis of the MC and controls the duty factor of the generated parametric pulses only at the MC forbidden frequency.

**Keywords:** dissipative solitons, magnonic crystals, spin waves.

DOI: 10.21883/TPL.2023.04.55871.19509

The examination of wave and oscillatory processes in ferromagnetic micro- and nanostructures has attracted a significant amount of interest in recent years both in Russia and abroad [1–3]. Driven by the progress in spintronics, the research into direct-current control over these processes has stimulated the development of a new discipline: magnon spintronics [4]. It is known that dynamic control over magnons (quanta of spin waves, SWs) may be effected either via their interaction with a spin-polarized current, which is induced in metal and non-metal ferromagnetic materials due to the spin Hall effect [5,6], or by altering the internal magnetic field of a ferromagnetic with the use of an external constant electric current [7,8].

The principle of dynamic control over magnons with the use of a constant electric current forms the basis of operation of a new spin-wave device called a dynamic magnonic crystal (DMC) [9,10]. It is known that a magnonic crystal (MC) is a magnetic material with a periodic structure, which acts similarly to the one in a photonic crystal and induces the formation of stop bands (bandgaps) satisfying the Bragg condition. In contrast to static MCs, DMCs feature bandgaps in the SW spectrum with their characteristics depending on a constant electric current. Thus, varying the current magnitude or polarity, one may control the level of losses at DMC bandgap frequencies. This dynamic SW loss control indicates that DMCs may be used to establish direct-current control over signal generation modes in active ring resonators.

Static magnonic crystals [11] and quasicrystals [12] supporting three-wave parametric decay of a magnetostatic surface (MSSW) have been used by now in microwave active ring resonators as nonlinear filters for the generation of chaotic bright dissipative envelope solitons. An adjustable attenuator was used to control the modes of generation of

these parametric pulses. Ultrashort (subnanosecond) dark dissipative envelope solitons have been produced in recent years in microwave active ring resonators with two nonlinear elements [13]. One of them was an irregular (curved) magnonic waveguide supporting three-wave parametric decay of a magnetostatic SW, and the other element was a transistor amplifier operated with output power saturation. Soliton modes were also controlled mechanically in this case. Research results demonstrating dynamic control over the duty factor of chaotic dark dissipative envelope solitons with the use of a constant electric current are reported below.

Figure 1 presents the diagram of an active ring resonator containing a one-dimensional (1D) MC with a dynamic linear defect, an amplifier cascade featuring three amplifiers, and an adjustable attenuator. The 1DMC was fabricated from an yttrium iron garnet (YIG) film with a thickness of  $10\mu\text{m}$ , a width of  $4\text{mm}$ , a length of  $10\text{mm}$ , and a saturation magnetization of  $1750\text{G}$ . A periodic structure in the form of columns and troughs with a period of  $200\mu\text{m}$  was patterned on the YIG film surface via etching and lithography. These columns and troughs had the same width:  $100\mu\text{m}$ . Troughs were etched to a depth of  $1\mu\text{m}$ . The periodic structure was  $4\text{mm}$  in length. A dynamic linear defect was produced by a constant electric current flowing along a copper wire  $100\mu\text{m}$  in diameter and  $4.5\text{mm}$  in length, which was positioned along the longitudinal symmetry axis of the 1DMC. The distance from the wire to the YIG film surface was  $100\mu\text{m}$ ; therefore, the influence of heating on the propagation of a magnetostatic SW could be excluded. Depending on the current polarity, the internal magnetic field of the 1DMC in the region of a wire conductor may either increase or decrease. Input and output microstrip transducers were used to excite and receive an

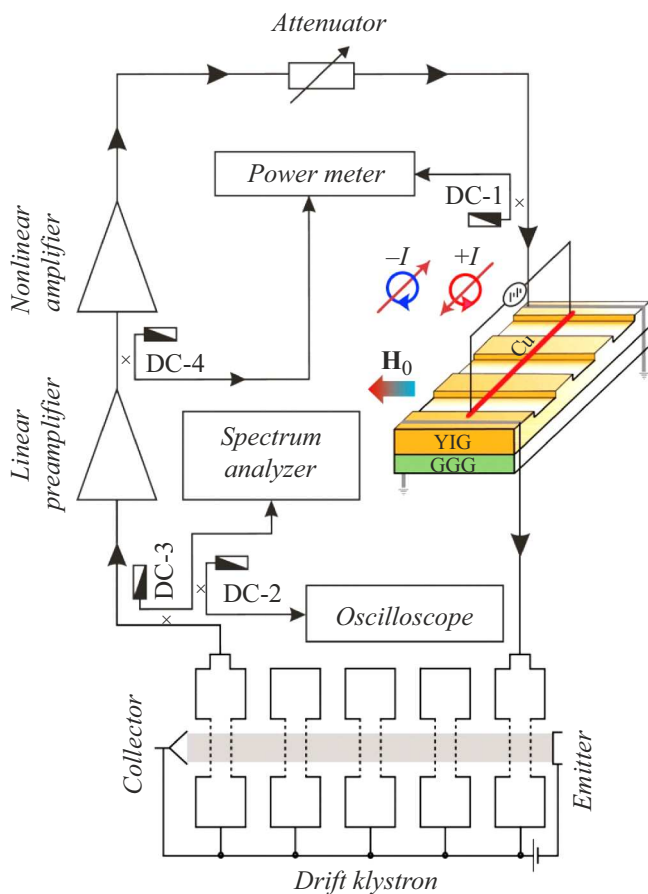


**Figure 1.** Block diagram of the microwave ring generator of chaotic dark dissipative envelope solitons.

MSSW propagating in the 1D MC. Each of them had a width of  $30\ \mu\text{m}$  and a length of 6 mm. The distance between them was 6 mm. External constant magnetic field  $H_0$  was applied tangentially to the 1D MC surface and parallel to microstrip transducers. Field intensity  $H_0 = 356\ \text{Oe}$  was chosen so as to establish the conditions for development of a three-wave parametric MSSW decay.

The amplifier cascade featured an amplifier klystron and two transistor amplifiers, which are needed to compensate for losses in the bandgap of the 1D MC. The output amplifier of the cascade was operated in the output power saturation mode, and the other two amplifiers were operated in the linear amplification mode. The amplifier klystron, which is a resonance-type amplifier with a central frequency of  $\sim 2.8\ \text{GHz}$ , was tuned to the vicinity of the central frequency of the 1D MC bandgap. The power level of the 1D MC input signal was set with the use of an adjustable attenuator. A microwave signal generated in the ring was fed to the inputs of a spectrum analyzer and a real-time oscilloscope for analysis and subsequent processing.

Figure 2, *a* shows the frequency response of the 1D MC measured in the linear mode. It can be seen that the MSSW spectrum features a stop band (bandgap) with a central frequency ( $f_{01} = 2797\ \text{MHz}$ ) corresponding to the

frequency of the first Bragg resonance. Figure 2, *b* presents the dependences of the transfer factor of the 1D MC on its input signal power, which were measured at several different magnitudes of a constant electric current applied to a wire conductor. Three cases were considered: (1) current is not passed through the conductor; (2) positive-polarity current is passed through the conductor; (3) negative-polarity current is passed through the conductor. The results presented in Fig. 2, *b* demonstrate that dependence  $S_{21}(P_{in})$  measured without a constant electric current contains both linear and nonlinear sections. The threshold of 1D MC switching to nonlinear operation is at an input power of  $-15\ \text{dBm}$ . An MSSW then starts decaying parametrically into SWs. If a positive-polarity constant electric current is passed through a wire conductor, both the linear losses level and the nonlinear threshold grow. This is attributable to the enhancement of the internal magnetic field of the 1D MC in the region of current flow. If the current polarity is negative, the linear losses level and the nonlinear threshold decrease. This is due to the suppression of the internal magnetic field of the 1D MC in the region of current flow. Thus, applying constant electric currents of different polarity to a wire conductor, one may control the level of both linear and nonlinear MSSW losses at a fixed frequency by shifting the bandgap frequency of the 1D MC. With the chosen current polarities, the dynamic range of variation of linear losses is  $\sim 4\ \text{dB}$ , and the dynamic range of variation of the threshold power is  $\sim 2\ \text{dB}$ . It should be noted that a constant electric current has no appreciable effect on the levels of linear and nonlinear MSSW losses at frequencies located far from the bandgap.

Figure 3 presents the results obtained by introducing the 1D MC into a feedback loop of an active ring resonator. Time series were measured at ring gain factor  $G = K - A = 31\ \text{dB}$  ( $K$  is the amplifier cascade gain and  $A$  is the overall loss level in the ring). The integrated signal power at the 1D MC input is then  $P_{in} = +3\ \text{dBm}$ . This value is  $18\ \text{dBm}$  above the nonlinear threshold, and the output amplifier of the cascade is operated with deep output power saturation. It follows from the data presented in Fig. 3, *a* that a chaotic sequence of pulse packets with a duration of  $\sim 0.9\ \mu\text{s}$  forms without a constant current ( $I = 0$ ). Each packet features „dips“ in the form of dark pulses. Some of these „dips“ are dissipative dark envelope solitons with a duration of  $\sim 30\ \text{ns}$ , since their amplitude drops to zero; the other „dips“ correspond to dissipative grey envelope solitons (their amplitude does not decay strictly to zero). The repetition rate of chaotic pulse packets averaged over the realization length assumes a value of  $\sim 100\ \text{kHz}$  and corresponds to the self-modulation frequency of parametrically excited SWs produced as a result of the three-wave MSSW decay. The duty factor of this pulse sequence is  $q \sim 11$ . Short dark pulses within pulse packets have an averaged repetition rate of  $\sim 8\ \text{MHz}$ , which is typical of four-wave interactions.

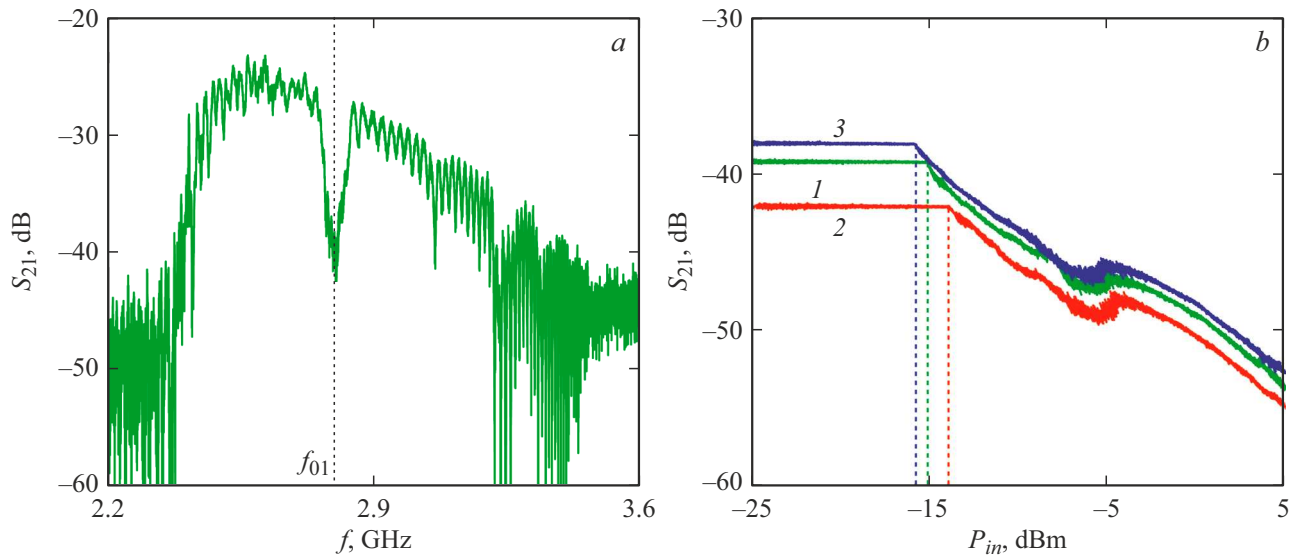


**Figure 2.** *a* — Frequency response of the 1D MC with a dynamic linear defect measured at  $P_{in} = -30$  dBm; *b* — dependences of the transfer factor of the 1D MC on  $P_{in}$  measured at the bandgap frequency at constant currents  $I = 0$  (1),  $+500$  (2), and  $-500$  mA (3).

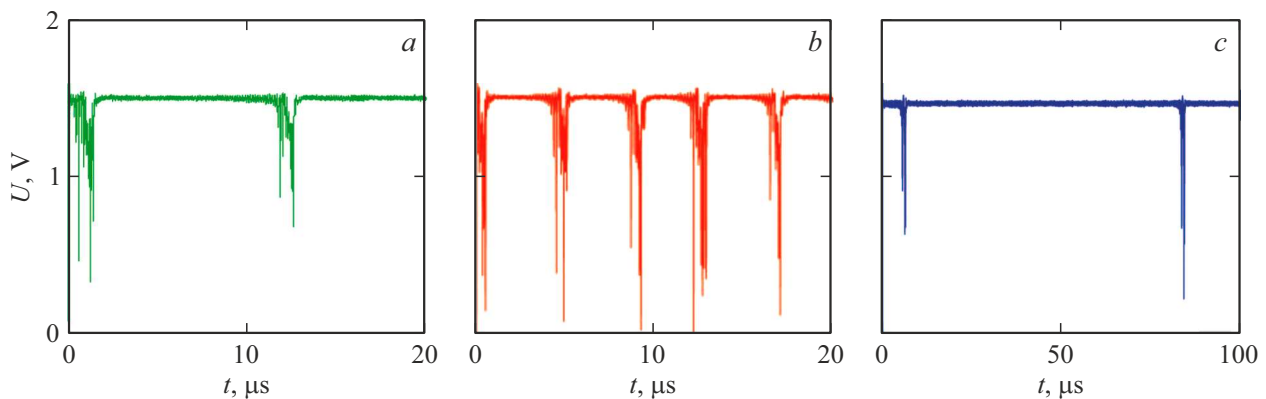


**Figure 3.** Chaotic sequences of dark dissipative envelope solitons obtained at constant electric currents  $I = 0$  (*a*),  $+320$  (*b*), and  $-200$  mA (*c*).

Figures 3, *b*, *c* show chaotic pulse sequences obtained by passing constant currents of different polarity through a wire conductor. It follows from the presented data that the SW self-modulation frequency increases to  $\sim 250$  kHz at a positive current polarity (the duty factor decreases to  $q \sim 4$ ); in contrast, the frequency drops to  $\sim 13$  kHz at a negative polarity (the duty factor increases to  $q \sim 80$ ). Thus, altering locally the internal magnetic field of the 1DMC via the application of a constant electric current of different polarities, one may control the duty factor of pulse sequences generated at the 1DMC bandgap frequency.

The obtained results may find application in the development of pulse signal sources for magnon logic and spintronic systems.

### Funding

This study was supported by a grant from the Russian Science Foundation (project No. 23-22-00274).

### Conflict of interest

The authors declare that they have no conflict of interest.

### References

- [1] P. Pirro, V.I. Vasyuchka, A.A. Serga, B. Hillebrands, *Nat. Rev. Mater.*, **6**, 1114 (2021). DOI: 10.1038/s41578-021-00332-w
- [2] S.A. Nikitov, A.R. Safin, D.V. Kalyabin, A.V. Sadovnikov, E.N. Beginin, M.V. Logunov, M.A. Morozova, S.A. Odintsov, S.A. Osokin, A.Yu. Sharaevskaya, Yu.P. Sharaevsky, A.I. Kirilyuk, *Phys. Usp.*, **63** (10), 945 (2020). DOI: 10.3367/UFNe.2019.07.038609.
- [3] *Three-dimensional magnonics. Layered, micro- and nanostructures*, ed. by G. Gubbiotti (Jenny Stanford Publ., N.Y., 2019). DOI: 10.1201/9780429299155
- [4] A.V. Chumak, V.I. Vasyuchka, A.A. Serga, B. Hillebrands, *Nat. Phys.*, **11** (6), 453 (2015). DOI: 10.1038/nphys3347

- [5] M. Tsoi, A.G.M. Jansen, J. Bass, W.-C. Chiang, M. Seck, V. Tsoi, P. Wyder, *Phys. Rev. Lett.*, **80** (19), 4281 (1998). DOI: 10.1103/PhysRevLett.80.4281
- [6] Y. Kajiwara, K. Harii, S. Takahashi, J. Ohe, K. Uchida, M. Mizuguchi, H. Umezawa, H. Kawai, K. Ando, K. Takanashi, S. Maekawa, E. Saitoh, *Nature*, **464** (11), 262 (2010). DOI: 10.1038/nature08876
- [7] S.O. Demokritov, A.A. Serga, A. Andre, V.E. Demidov, M.P. Kostylev, B.A. Hillebrands, N. Slavin, *Phys. Rev. Lett.*, **93** (4), 047201 (2004). DOI: 10.1103/PhysRevLett.93.047201
- [8] K. Vogt, F.Y. Fradin, J.E. Pearson, T. Sebastian, S.D. Bader, B. Hillebrands, A. Hoffmann, H. Schultheiss, *Nat. Commun.*, **5**, 3727 (2014). DOI: 10.1038/ncomms4727
- [9] A.V. Chumak, T. Neumann, A.A. Serga, B. Hillebrands, M.P. Kostylev, *J. Phys. D: Appl. Phys.*, **42** (20), 205005 (2009). DOI: 10.1088/0022-3727/42/20/205005
- [10] A.A. Nikitin, A.B. Ustinov, A.A. Semenov, A.V. Chumak, A.A. Serga, V.I. Vasyuchka, E. Lähderanta, B.A. Kalinikos, B. Hillebrands, *Appl. Phys. Lett.*, **106** (10), 102405 (2015). DOI: 10.1063/1.4914506
- [11] S.V. Grishin, Yu.P. Sharaevskii, S.A. Nikitov, E.N. Beginin, S.E. Sheshukova, *IEEE Trans. Magn.*, **47** (10), 3716 (2011). DOI: 10.1109/TMAG.2011.2158293
- [12] S.V. Grishin, O.I. Moskalenko, A.N. Pavlov, D.V. Romanenko, A.V. Sadovnikov, Yu.P. Sharaevskii, I.V. Sysoev, T.M. Medvedeva, E.P. Seleznev, S.A. Nikitov, *Phys. Rev. Appl.*, **16** (5), 054029 (2021). DOI: 10.1103/PhysRevApplied.16.054029
- [13] A.S. Bir, S.V. Grishin, O.I. Moskalenko, A.N. Pavlov, M.O. Zhuravlev, D. Osuna Ruiz, *Phys. Rev. Lett.*, **125** (8), 083903 (2020). DOI: 10.1103/PhysRevLett.125.083903